J Mater Sci (2008) 43:6070–6080
DOI 10.1007/s10853-008-2956-8

A generalisation of the Wilshire–Scharning methodology to creep life prediction with application to 1Cr–1Mo–0.25 V rotor steel

M. Evans

Received: 3 July 2008 / Accepted: 14 August 2008 / Published online: 4 September 2008

Abstract Wilshire–Scharning have recently developed a new methodology that has been demonstrated to deliver accurate longer term creep life predictions, and so offers the prospect of cost-effective acquisition of long-term creep design data. This methodology differs from existing approaches to creep life prediction by normalising the applied stress through the appropriate tensile strength. This article develops a generalisation of this Wilshire–Scharning model that has the potential to increase the predictive accuracy of this methodology—which will be so essential if it is to be adopted as a way of economising on the acquisition of creep design data. When applied to 1Cr–1Mo–0.25 V steel, it was found that this generalisation reduced the average error in prediction from 2.5 under the Wilshire–Scharning specification to 1.8 years when extrapolating from 5,000 out to over 100,000 h. Further, over this time scale the generalised model produces a mean absolute percentage error of 28%. This compares to 47% obtained using the traditional 4Θ projection technique and 26% using a modification of this methodology as recently proposed by Evans.

Introduction

Large-scale components and structures for power plants are usually designed on the basis that creep failure should not occur during planned lives of around 30 years. Such decisions are generally based on the allowable tensile creep strengths. In most cases there is no derivation of statistical confidence intervals so that these strengths are often determined as 80% of the minimum stress causing rupture in 100,000 h. Because of this extended time frame the creation of a comprehensive database for any new power plant steel then represents a very expensive and protracted task.

The large timescales involved in such testing only account for part of the testing cost. In response to the well-known batch-to-batch scatter present even in steels that are within specified compositional limits, the international standard ISO 6303 requires the completion of tests lasting up to 30,000 h over the relevant temperature ranges for five melts of each grade [1, 2]. In addition, for several newly developed steels, the allowable strengths have been progressively reduced as measurements from longer term tests have become available [3–5]. These and other studies have emphasised the limitations of existing methods for data extrapolation from short-term tests.

These and other uncertainties have then justified the completion of protracted programmes covering stress–temperature conditions giving creep lives up to 100,000 h or more for multiple batches of many power plant steels [2]. Against this background, Wilshire and Scharning [6–9] have recently developed a new methodology offering the prospect of cost effective acquisition of long-term creep design data. Using a variety of different materials, these authors have demonstrated that by normalising the applied stress through the appropriate tensile strength, the methodology is capable of accurately predicting, from relatively short-term data, the minimum creep rates, the times to various strains and the creep lives for stress–temperature conditions causing failure in 100,000 h and more. Evans [10] has also recently demonstrated the predictive superiority of this methodology over existing extrapolation

M. Evans (✉)
School of Engineering, Swansea University, Singleton Park, Swansea SA2 8PP, UK
e-mail: m.evans@swansea.ac.uk

procedures using 1Cr–1Mo–0.25 V steel as a test-bed material. These authors have also demonstrated that such normalisation results in a substantial reduction in the batch-to-batch scatter.

This article provides a generalisation of this methodology that has the potential to further improve the accuracy of creep life predictions obtainable under this new methodology. This is an important objective, because if the methodology of normalising the stress is to be adopted as a way of economising on the acquisition of long-term creep design data, demonstrative accuracy over a wide range of materials is an essential prerequisite. The proposed generalisation is then applied to data on 1Cr–1Mo–0.25 V steel and relative predictive accuracies quantified.

To meet this objective, this article is structured as follows. The following section describes the data set used for illustrating the use of the generalised model. This is followed by a section that outlines a generalisation of the Wilshire–Scharning model and which also looks at issues related to how such a generalised model is estimated and then used to obtain long-term creep life predictions. The next section then describes how predictive accuracy can be sensibly measured and the applications section shows the estimated parameters of the generalised model, together with some lifetime predictions. Predictions from the Wilshire–Scharning model, variations of the Θ projection technique and the generalised models are then compared. A concluding section will then outline some proposals for future work.

The data

For illustrative purposes, this article features forged 1Cr–1Mo–0.25 V steel for turbine rotors and shafts. For multiple batches of this bainitic product, both the creep and creep fracture properties have been documented comprehensively by the National Institute for Materials Science (NIMS), Japan [11]. NIMS creep data sheet No. 9B includes information on nine batches of as tempered 1Cr–1Mo–0.25 V steel. Table 1 gives the chemical composition of each of these batches. Specimens for the tensile and creep rupture tests were taken radially from the ring-shaped samples which were removed from the turbine rotors. Each test specimen had a diameter of 10 mm with a gauge length of 50 mm.

These specimens were tested at constant load (τ) over a wide range of conditions: 333–47 MPa and 723–923 K. In addition to minimum creep rate ($\dot{e}_m$) and time to failure (t_F) measurements, listings were also given of the times to attain various strains (t_e) at 0.005, 0.01, 0.02 and 0.05 over this range of test conditions. Also reported were the values of the 0.2% proof stress (τ_Y) and the ultimate tensile strength (τ_{TS}) determined from high strain rate ($\sim 10^{-3}$ s^{-1}) tensile tests carried out at the creep temperatures for each batch of steel investigated. Using this freely available NIMS document, the accuracy with which 100,000 h strengths can be estimated by extrapolation of short-term results can be assessed against reliable long-term measurements.

Proposed generalisation of the Wilshire–Scharning model

The Wilshire–Scharning model

Wilshire and Scharning [6–9] have recently suggested that the applied stress should be normalised through measured values of ultimate tensile strength so that data sets can be considered over the complete stress range for $\tau/\tau_{TS} = 1$ to 0. Valid relationships devised to quantify creep rupture measurements must then make it evident not only that $t_F \to 0$ as $\tau/\tau_{TS} \to 1$, but also that $t_F \to \infty$ as $\tau/\tau_{TS} \to 0$. Whilst many formulations of this are possible, Wilshire and Scharning opted for the following functional form

Table 1 Composition and heat treatment of 1Cr–1Mo–0.25 V steel

Batch code Requirements	Chemical composition (mass %)											
	C 0.25–0.35	Si 0.15–0.35	Mn ≤1.0	P ≤0.015	S ≤0.018	Ni ≤0.75	Cr 0.9–1.5	Mo 1.0–1.05	Cu –	V 0.2–0.3	Al –	N –
VaA	0.28	0.20	0.72	0.015	0.012	0.32	1.02	1.12	0.20	0.27	0.002	0.0075
VaB	0.28	0.18	0.75	0.012	0.009	0.32	1.00	1.25	0.14	0.26	0.002	0.009
VaC	0.29	0.20	0.75	0.010	0.009	0.34	1.00	1.25	0.14	0.26	<0.002	0.0075
VaD	0.3	0.28	0.72	0.014	0.006	0.35	0.93	1.22	0.16	0.21	0.002	0.0093
VaE	0.3	0.26	0.79	0.016	0.015	0.32	1.03	1.13	0.19	0.23	<0.002	0.0085
VaG	0.29	0.26	0.76	0.009	0.007	0.45	1.12	1.18	0.07	0.23	0.002	0.0103
VaH	0.29	0.26	0.77	0.009	0.007	0.46	1.12	1.20	0.08	0.23	<0.002	0.0095
VaJ	0.29	0.21	0.66	0.010	0.008	0.51	1.07	1.29	0.06	0.23	0.002	0.0097
VaR	0.3	0.27	0.70	0.012	0.012	0.44	1.10	1.35	0.11	0.27	0.002	0.0082

$$\tau/\tau_{TS} = \exp\left\{-k_1\left[t_F \exp\left(-Q_c^*/RT\right)\right]^u\right\}, \quad (1a)$$

where Q_c^* is the activation energy for lattice self-diffusion in the alloy steel matrixes, R the universal gas constant (8.314 J mol^{-1} K^{-1}), T the absolute temperature and k_1 and u are parameters that will require estimation. In Eq. 1a, τ/τ_{TS} varies from 1 to 0 in an S-shaped fashion as $t_F \exp\left(-Q_c^*/RT\right)$ varies from 0 to ∞. The precise shape of this sigmoidal function then depends on the value of u.

A generalisation of the Wilshire–Scharning model

A clue as to the best way to generalise this sigmoidal function comes from realising that the functional form of Eq. 1a is in fact the same as that for the cumulative density function (CDF) of a variable that follows a Weibull distribution. Just as τ/τ_{TS} must lie in the 0–1 range, so too must the cumulative probability, p. If a variable x follows a Weibull distribution, then its CDF is given by

$$p = \exp[-(\lambda_0 x)^u]. \quad (1b)$$

Now if the variable x is given by

$$x = t_F \exp\left(-Q_c^*/RT\right) \quad (1c)$$

then Eqs. 1a and 1b are identical with $k_1 = (\lambda_0)^u$ and with p being synonymous with τ/τ_{TS}.

This Weibull CDF is in turn a special case of the generalised F distribution [12] and so it is entirely sensible to consider this as the logical generalisation of the Wilshire–Scharning model. The CDF for the generalised F distribution is

$$p = I(s, m_1; m_2) \quad \text{with} \quad s = [1 + (m_1/m_2 e^w)]^{-1}, \quad (2a)$$

where $I()$ is the incomplete beta integral that depends upon the values of s, m_1 and m_2 and it can be calculated using the results of Abramowitz and Stegan [13]. m_1 and m_2 are two additional parameters that in part determine the shape of this sigmoidal function and

$$w = \frac{1}{\sigma\delta}\ln[x] - \frac{\mu}{\sigma\delta} \quad \text{with} \quad \delta = \sqrt{\frac{m_1 m_2}{m_1 + m_2}}. \quad (2b)$$

In order to see how this relates to the original Wilshire–Scharning model considers some special cases. When $m_2 = \infty$, the model simplifies to the generalised gamma distribution. The CDF for the generalised gamma distribution is

$$p = Q(m_1, s) \quad \text{with} \quad s = m_1 e^{w/\delta}, \quad (3a)$$

where $Q()$ is the incomplete gamma integral that can also be calculated using the results of Abramowitz and Stegan [13], and

$$w = \frac{1}{\sigma\delta}\ln[x] - \frac{\mu}{\sigma\delta} \quad \text{with} \quad \delta = \sqrt{m_1}. \quad (3b)$$

Then when $m_1 = 1$ with $m_2 = \infty$, Eqs. 3a and 3b collapse to

$$p = \exp[-e^w] \quad \text{where} \quad w = \frac{1}{\sigma}\ln[x] - \frac{\mu}{\sigma}. \quad (4)$$

A proof of these simplifications can be found in Prentice [14]. Equation 4 is now identical to the Wilshire–Scharning model given by Eq. 1a with $p = \tau/\tau_{TS}$, $u = 1/\sigma$ and $k_1 = (e^{-\mu})^u$. With two additional parameters in m_1 and m_2, Eqs. 2 allows for more flexibility in describing the functional relationship between τ/τ_{TS} and x. This is illustrated in Fig. 1. The solid curve shows the shape of the Wilshire–Scharning model when $\mu = 0$ and $\sigma = 1$ (i.e. when $k_1 = 1$ and $u = 1$). The other two curves then illustrate the extra variation in shape that the generalised sigmoidal allows as a results of having the two additional parameters m_1 and m_2. Variations in σ will result in further changes in the shape of these sigmoidal curves. μ is simply a scaling parameter.

The Wilshire–Scharning model was first published in a paper studying polycrystalline copper [6]. In this article, the authors found that the parameters of Eq. 1a differed at stresses above and below the yield stress. Rather than attributing this to a mechanism change, they provided evidence to suggest that this was attributable to grain deformation as the movement of dislocations becomes progressively less important as deformation is increasingly confined to grain boundary zones as stress falls below the yield stress. Since then, Wilshire and Scharning have found similar 'kinks' in 1Cr–1Mo–0.25 V and 9–12% chromium steels [7, 8] and some Al alloys [9].

As demonstrated by Evans [10], one way to formalise such a kink is through the use of a spline function. These are continuous functions that allow for such differing parameter values. Using such a spline function, a kink can be incorporated into the Wishire–Scharning model as follows

$$\tau^* = -\ln(k_1) + (u)\ln(x) + a[\ln(x) - x_0^*]D, \quad (5)$$

where $\tau^* = \ln(-\ln(\tau/\tau_{TS}))$, x^*_0 is the value for $\ln(x)$ at which u and k_1 change and $D = 0$ when $[\ln(x) - x_0^*] \leq 0$ and $D = 1$ otherwise. Within the framework, x_0^* and a should be seen as further parameters whose value should be determined from the data. So before the change when $D = 0$

$$\tau^* = -\ln(k_1) + (u)\ln(x)$$

but after the change when $D = 1$

$$\tau^* = \{-\ln(k_1) - ax_0^*\} + [u + a]\ln(x).$$

This kink can also be introduced into the generalised model by rewriting Eq. 2b as

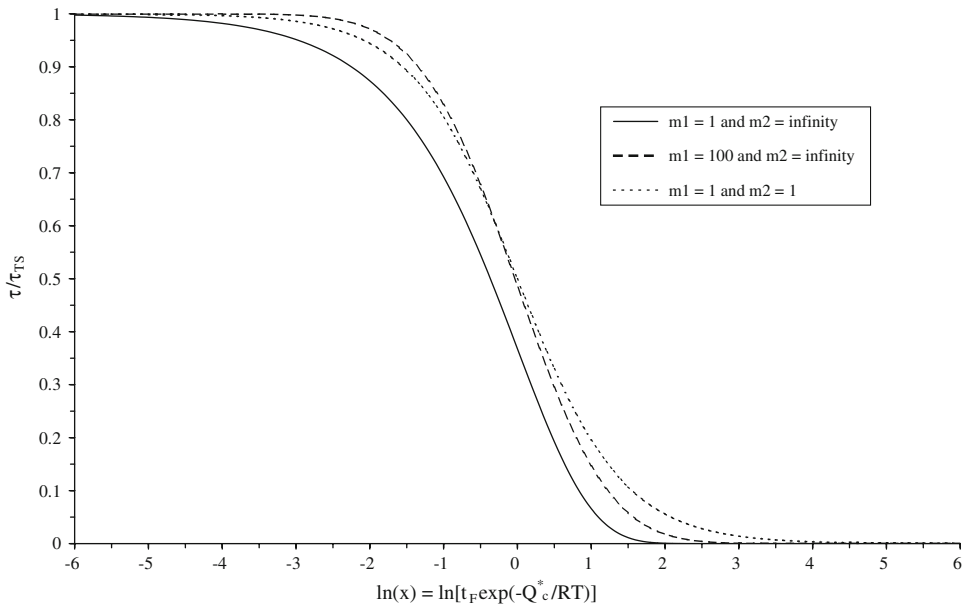

Fig. 1 The generalised sigmoidal traced out for various values of m_1 and m_2 with $\mu = 0$ and $\sigma = 1$ in Eqs. 2

$$w = \frac{1}{\sigma\delta}\ln[x] - \frac{\mu}{\sigma\delta} + a[\ln(x) - x_0^*]D, \tag{6}$$

where $w = \tau^*$ and $\delta = 1$ when $m_1 = 1$ with $m_2 = \infty$, making Eqs. 5 and 6 equivalent in this special case of the generalised model (with $1/\sigma = u$ and $\mu/\sigma = \ln(k_1)$).

The generalised model expressed in Excel

Although at first sight this generalisation looks rather complicated to implement, due to the lack of closed form expressions, it is in fact very straightforward to apply in Excel. Figure 2 is a screen caption illustrating such an implementation for a single observation on x. Cells B7:D7 contain the results for one specimen tested on the NIMS programme. Cell G7 works out the temperature compensated failure time, x, and its natural log is calculated in cell H7. Cells I7:K7 define and calculate the variables w and s in Eqs. 2a and 2b. Then in cell L7 the predicted value for τ/τ_{TS} is given. The Excel function BETADIST gives the CDF of the beta distribution as a function of s, which is in fact the incomplete beta integral $I()$ of Eq. 2a. These values are all worked out for the parameter values shown in cells E3:L3.

Notice that in this illustration, $m_1 = 1$ and m_2 is very large so that the resulting predicted value for τ/τ_{TS} is that which would be given by the Wilshire–Scharning model

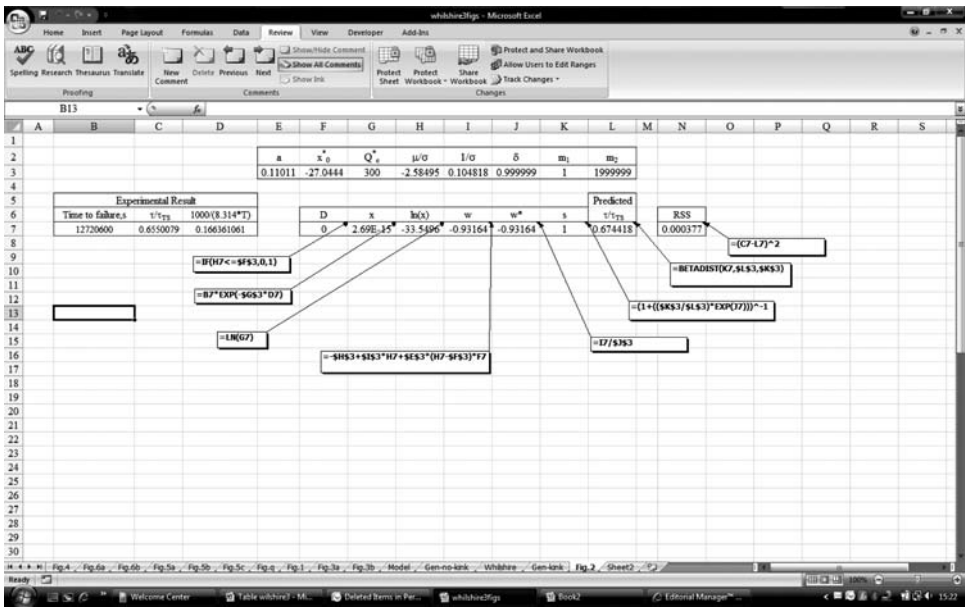

Fig. 2 Excel implementation of the generalised model given by Eqs. 2a and 6

with $k_1 = 13.26$ and $u = 0.11$ when $\ln(x)$ is ≤ -27 and with $k_1 = 260$ and $u = 0.21$ when $\ln(x)$ is > -27. Then in cell N7 the squared difference between the actual normalised stress and that predicted by the model is worked out. This so-called squared residual can be used to determine the values given for the parameters of the model shown in cells E3:L3 in the way described in the following section.

Estimating the parameters of the generalised model

A squared residual can be worked out for each and every test condition i (of which there are n_1), and the sum of these residuals can then be calculated as

$$\mathrm{RSS} = \sum_{i=1}^{n_1} \left[(\tau/\tau_{\mathrm{TS}})_i - (\tau/\tau_{\mathrm{TS}})_i^p \right]^2, \tag{7}$$

where $(\tau/\tau_{\mathrm{TS}})^p$ is the models prediction of τ/τ_{TS}. It then makes sense to chose parameter values that minimise this so-called residual sum of squares, because the values for τ/τ_{TS} predicted by the model are as close as possible to the experimental values.

In this research article, a two-step optimisation procedure is used. First, a value for m_1 and m_2 is selected. Then values for μ and σ are then chosen so as to minimise Eq. 7 for these given values of m_1 and m_2. This is a nonlinear least squares optimisation procedure that can be easily carried out in Excel using the Solver option or using well-known algorithms such as those documented in Brendt et al. [15]. This process is repeated for a variety of values for m_1 and m_2, giving a variety of different minimised RSS. The optimised values for μ, σ, m_1 and m_2 correspond to those which give the smallest of these minimised RSS. Under this two-stage procedure only μ and σ will have a standard error associated with them.

Then provided that the individual $(\tau/\tau_{\mathrm{TS}})_i - (\tau/\tau_{\mathrm{TS}})_i^p$ is normally distributed, those values for m_1 and m_2 that are supported by the data at the 5% significance level will have a value of <3.81 for the following test statistic

$$\chi^2_{1,j} = n_1 \left[\mathrm{RSS}_j - \min(\mathrm{RSS}) \right]. \tag{8}$$

In Eq. 8, RSS_j is the residual sum of squares associated with the jth values for m_1 and m_2, min(RSS) is the smallest RSS over all j values for m_1 and m_2, and n_1 is the sample size used to estimate the parameters μ, σ, m_1 and m_2.

Obtaining failure time predictions from the generalised model

Because the generalised model has no closed form expression, except for a few special cases such as the Wilshire–Scharning model, failure time predictions require a numerical solution to the equation

$$\tau/\tau_{\mathrm{TS}} = I(s, m_1; m_2). \tag{9}$$

In Eq. 9, τ/τ_{TS} is the actual normalised stress corresponding to a particular test condition. A value for t_{F} and thus s, for given values of m_1 and m_2, that sets $I(s, m_1; m_2)$ equal to this actual normalised stress can then be found numerically. This is very straightforward to do in Excel using its Goal seek function.

Measuring predictive accuracy

The following is a proposed acid test of extrapolation that any creep life prediction model can be subjected to. First, a long-term creep data set should be split into two parts (A and B) using an arbitrary split defined in terms of a short-term time to failure. Data set A will then be made up of $i = 1$, n_1 specimens, whilst data set B will made up of $i = 1$, n_2 specimens. The parameters of each model should then be chosen so that the model best fits the data in part A—i.e. minimises the residual sum of squares. The estimated models should then be used to predict the times at which the specimens failed in data set B. It is proposed that the accuracy of these predictions be assessed using an actual versus prediction regression of the form

$$t_{\mathrm{F}_i} = \hat{\alpha}_0 + \hat{\alpha}_1 \hat{t}_{\mathrm{F}_i} + e_i \quad i = 1, n_2, \tag{10a}$$

where t_{F_i} and $\hat{t}_{\mathrm{F}_i}$ are the actual and predicted times to failure under test condition i of the creep data set B. $\hat{\alpha}_0$ and $\hat{\alpha}_1$ are the least squares estimates of the intercept and slope, respectively, of the best-fit line through the $t_{\mathrm{F}_i} - \hat{t}_{\mathrm{F}_i}$ pairings. A perfect model would then correspond to $\hat{\alpha}_0 = 0$, $\hat{\alpha}_1 = 1$ and $e_i = 0$ for all i. Interestingly, Theil [16] has related Eq. 10a to a more familiar measure of predictive accuracy—the mean square error (MSE)

$$\mathrm{MSE} = \frac{1}{n_2} \sum_{i=1}^{n_2} \left[t_{\mathrm{F}i} - \hat{t}_{\mathrm{F}i} \right]^2, \tag{10b}$$

where the sum is over all n_2 specimens making up the creep data set B. Theil [16] has shown that the MSE can be decomposed into the following three parts

$$\mathrm{MSE} = \left[\bar{t}_{\mathrm{F}} - \bar{\hat{t}}_{\mathrm{F}} \right]^2 + \left\{ (\hat{\alpha}_1 - 1)^2 S^2_{\hat{t}_{\mathrm{F}}} \right\} + S_e^2, \tag{10c}$$

where $S^2_{\hat{t}_{\mathrm{F}}}$ is the variance of the failure time predictions, S_e^2 is the variance of e in Eq. 10a and $\bar{t}_{\mathrm{F}}$ the average failure time over the n_2 tests. Further, when $\hat{\alpha}_1 = 1$, $[\bar{t}_{\mathrm{F}} - \bar{\hat{t}}_{\mathrm{F}}] = \hat{\alpha}_0$. Thus $\mathrm{UM} = [\bar{t}_{\mathrm{F}} - \bar{\hat{t}}_{\mathrm{F}}]^2/\mathrm{MSE}$ is the proportion of the MSE due to a mean prediction error. But when $\hat{\alpha}_1 \neq 1$ the

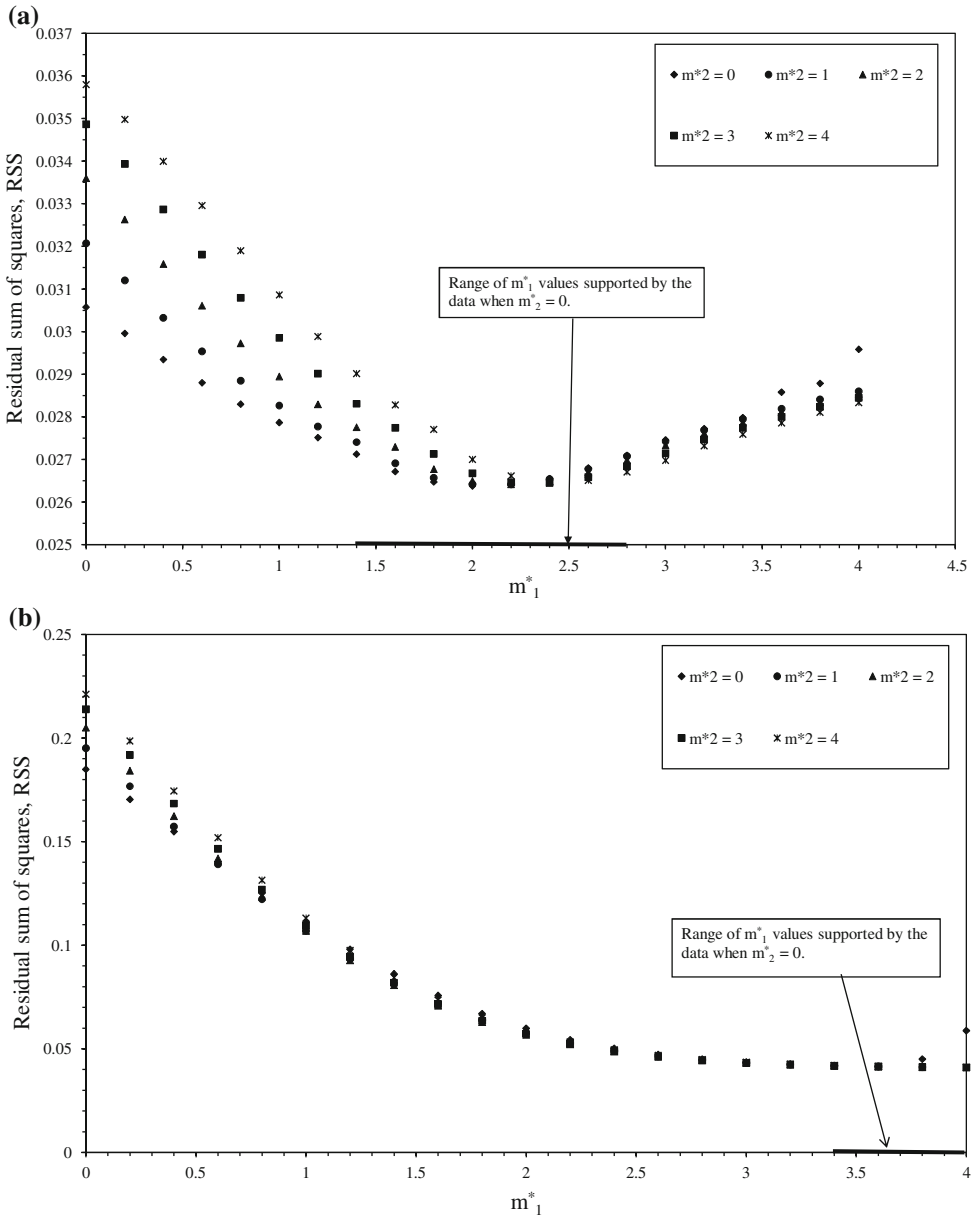

Fig. 3 Residual sum of squares plotted against various values for m_1^* and m_2^* for the generalised model with (**a**) a kink included as given by Eqs. 2a and 6 and (**b**) no kink included as given by Eqs. 2a and 2b

average prediction error depends on both $\hat{\alpha}_0$ and $\hat{\alpha}_1$ through the expression $[\bar{t}_F - \bar{\hat{t}}_F] = \hat{\alpha}_0 + (\hat{\alpha}_1 - 1)\bar{\hat{t}}_F$. Further, UR = UR $= \left\{(\hat{\alpha}_1 - 1)^2 S^2_{\hat{t}_F}\right\} \Big/ \text{MSE}$ is the proportion of the MSE due to the slope coefficient in Eq. 10a differing from 1. UM and UR therefore clearly represent systematic errors and large values for these two terms are a strong indication that the creep life prediction model is misspecified in some way. Finally, UD $= S_e^2/\text{MSE}$ is the proportion of the MSE which is unexplained by the mean or slope error and can be interpreted as being random in nature. The MSE error is therefore made of random and systematic prediction errors and the best model will have a small systematic component.

Application of the generalised model to 1Cr–1Mo–0.25 V steel

Using the terminology of the section 'Measuring predictive accuracy', Part A of the NIMS data set described in the section 'The data' contains all those specimens that failed at or before 5,000 h with part B being made up of all those specimens failing beyond 5,000 h. Data set A is therefore made up of $i = 1$, $n_1 = 119$ specimens, whilst data set B was made up of $i = 1$, $n_2 = 110$ specimens. Figure 3 shows the results of estimating the generalised model for various values of m_1 and m_2 using only the information contained in data set A. In these figures the values for m_1

and m_2 have been transformed along the lines suggested by Prentice [14] using

$$m_1^* = 2(m_1 + m_2)^{-1} \quad \text{and}$$
$$m_2^* = (m_1^{-1} - m_2^{-1})(m_1^{-1} + m_2^{-1})^{-1/2}$$

so that axis scales do not range from 0 to infinity. Within this simple transformation, the Wilshire–Scharning model corresponds to $m_1^* = 1$ and $m_2^* = 0$. In Fig. 3a the minimised residual sum of squares of the generalised model with a kink (i.e. Eqs. 2a and 6) obtained at various values for m_1^* and m_2^* is shown. As can be seen the best values for m_1^* and m_2^* are 2 and 0, respectively. When $m_2^* = 0$, the likelihood ratio statistic given by Eq. 8 rejects the Wilshire–Scharning model as a valid restriction at the 5% significance level ($\chi^2_{1,j} = 6.52$). Except at very small and large values for m_1^*, values for m_2^* have little effect on the residual sum of squares.

A similar picture emerges in Fig. 3b where the minimised residual sum of squares of the generalised model with no kink (i.e. Eqs. 2a and 2b) obtained at various values for m_1^* and m_2^* is shown. As can be seen the best values for m_1^* and m_2^* are 4 and 0, respectively. When $m_2^* = 0$, the likelihood ratio statistic given by Eq. 8 rejects the values for $m_1^* < 3.4$ as a valid restriction at the 5% significance level ($\chi^2_{1,j} = 118.86$). Thus the Wilshire–Scharning model with no kink is also not supported by the experimental data. Except at very small values for m_1^*, values for m_2^* have little effect on the residual sum of squares.

Table 2 shows the nonlinear least squares estimates for the generalised model (with and without a kink) corresponding to the optimal values for m_1 and m_2 shown in Fig. 3. These parameters were estimated using only data with failure times <5,000 h. Clearly, the residual sum of squares is smallest for the generalised model with a kink, but for both models all the parameters are statistically significant at the 5% significance level. When a kink is included in the model, the break occurs at a value of −27.6 for $x = t_F \exp\left(-Q_c^*/RT\right)$. Above the kink the value for $1/\sigma$ increases by 0.093 units compared to its below the kink value of 0.154. These two models, together with the Wilshire–Scharning model, are visualised in Fig. 4. All three models fit the data well—including the failure times above 5,000 h that the models have not 'seen'. These three models appear to give similar fits to the data, except around the kink point of $x = -27$ and at the extreme values for x. It is therefore arguable as to whether the extra complexity of introducing a kink into the model is required.

Table 2 Values for the parameters of Eqs. 2a and 2b and 2a and 6 estimated from specimen data that failed before $t_F = 5{,}000$ h using nonlinear least squares

Generalised models		
Parameter	Estimate (kink)	Estimate (no kink)
$*\mu/\sigma$	−3.463 [−21.9]	−9.236 [−77.2]
$*1/\sigma$	0.154 [29.6]	0.405 [87.5]
$*a$	0.093 [14.5]	n/a
$*x_0^*$	−27.616 [−132.0]	n/a
k_1	0.25 [−]	0.053 [−]
k_2	∞ [−]	0.947 [−]
RSS	0.0266	0.0409

* Indicates a variable that is statistically significant at the 5% level. Student t-values are in parenthesis. RSS, the residual sum of squares, − indicates no standard error associated with variable. n/a indicates that the corresponding variable is not part of the model

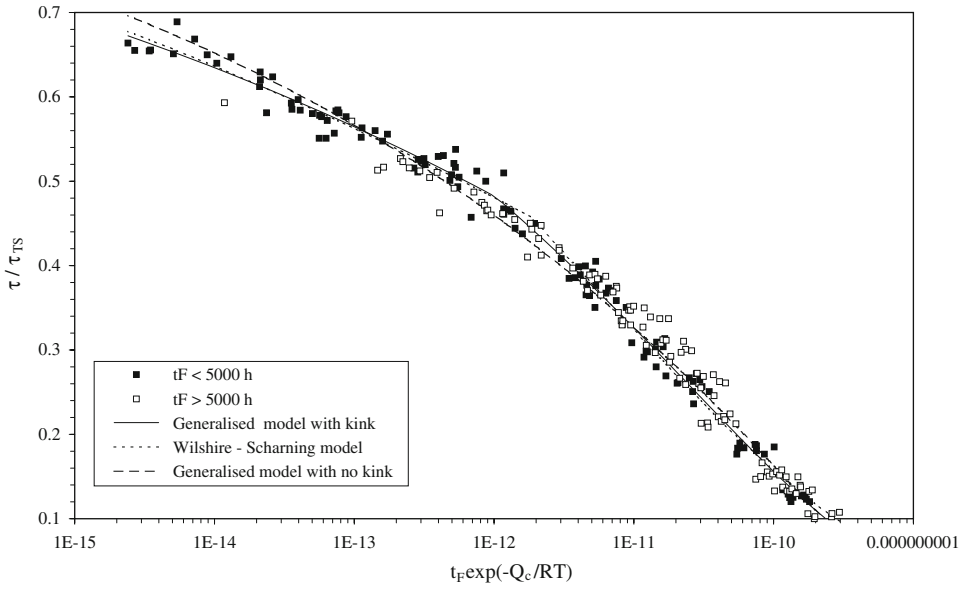

Fig. 4 Sigmoidal dependence of $t_F \exp\left(-Q_c^*/RT\right)$ on τ/τ_{TS} using Eqs. 2a and 6, 2a and 2b and 4 with $Q_c^* = 300\,\text{kJ mol}^{-1}$ for 1Cr–1Mo–0.25 V steel at 723–948 K

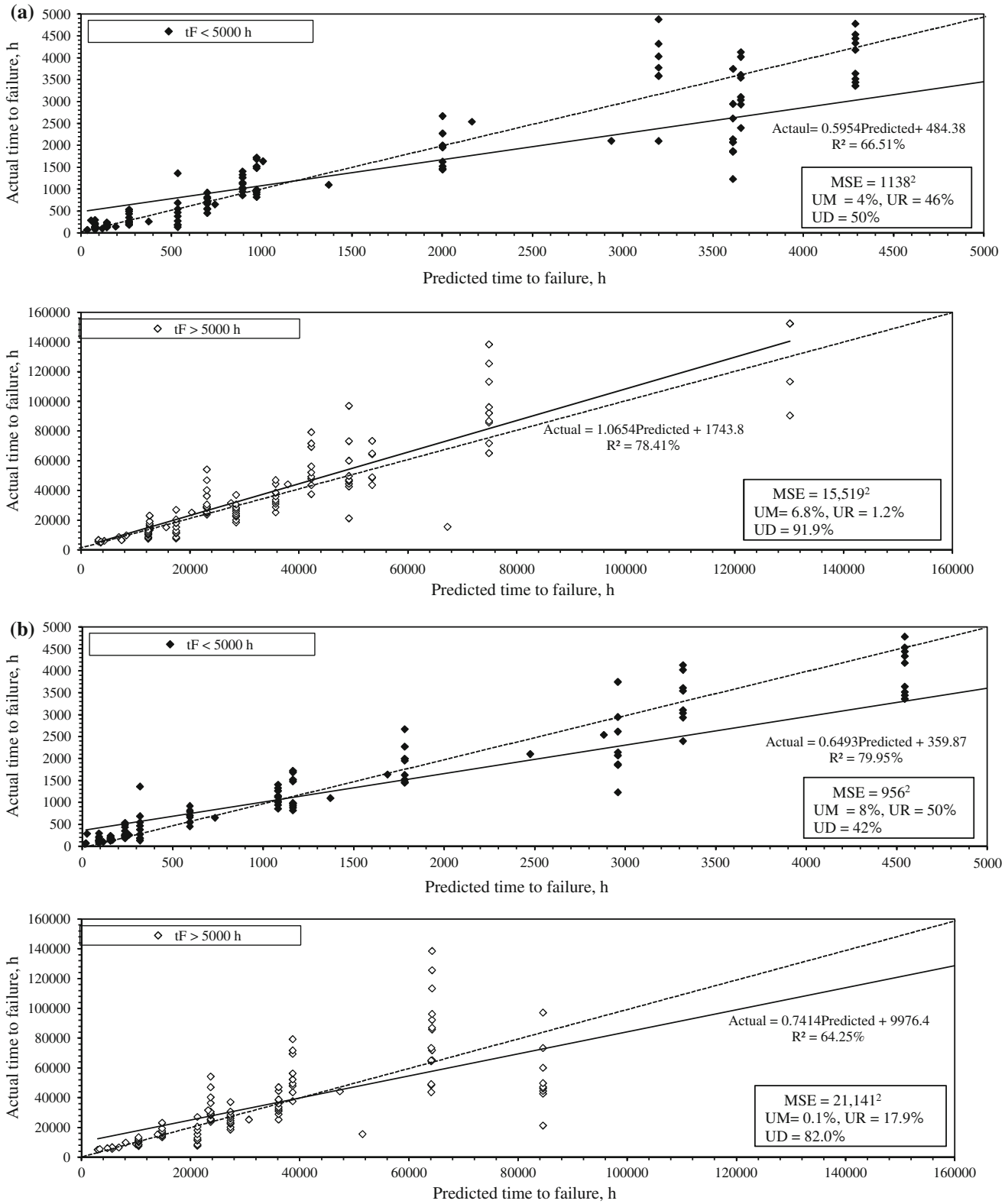

Fig. 5 Actual versus prediction plot for 1Cr–1Mo–0.25 V steel using the (**a**) generalised model with no kink given by Eqs. 2a and 2b, (**b**) Wilshire–Scharning model given by Eq. 4 (**c**) generalised model with a kink given by Eqs. 2a and 6

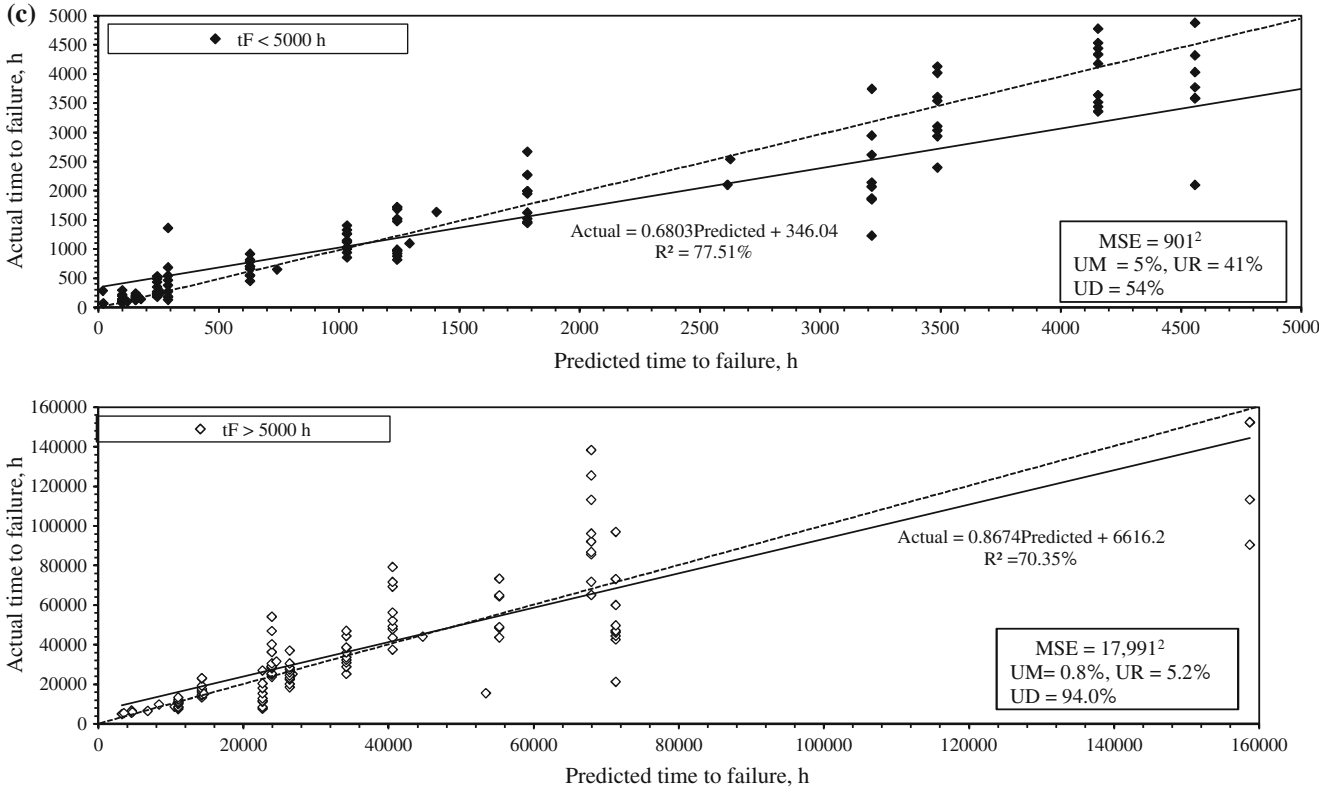

Fig. 5 continued

In order to assess the accuracy of the Wilshire–Scharning model relative to the generalised version (with and without a kink), Fig. 5 shows actual versus prediction plots for each model. The predictions shown in these figures were obtained using the median τ_{TS} (over all batches) at each temperature, rather than the actual τ_{TS} associated with each batch at each temperature. The top half of each of these figures shows the accuracies of the interpolations made by each model (each model was estimated from failure times <5,000 h). Each model gives a very similar performance with an MSE of around $1{,}000^2$. Also, for each model the random component of this MSE is around 50%, with most of the remaining systematic bias composing from the fact that the best-fit line on these plots has a slope <1. There is therefore some divergence from the optimum outcome given by the 45° line.

However, there is a big difference in their extrapolative performances, as shown by the bottom graphs in Fig. 5. The generalised model with no kink performed the best with a MSE of $15{,}519^2$. On average this model was in error by some 15,519 h or 1.8 years. Nearly 92% of this error was random in nature so that no real evidence of systematic error is present. The generalised model with a kink performed very similarly. However, the Wilshire–Scharning model gave an MSE of $21{,}141^2$. On average this model was in error by some 21,141 h or 2.5 years. The systematic component of this error was also higher than in the generalised model at some 18%.

It is also interesting to see how all these predictions look when plotted against the test stress, as in Fig. 6. In Fig. 6a, predictions from the generalised model with no kink are plotted together with the Wilshire–Scharning predictions. Where the Wilshire–Scharning longer term predictions are weakest (i.e. at 823 and 773 K), the predictions from the generalised model look better. It can also be noted that at the higher temperatures, the two models produce very different prediction profiles at the lower stresses, with the Wilshire–Scharning model giving much more optimistic life times at these stresses. A similar picture emerges in Fig. 6b although now the differences in the predictions produced by the Wilshire–Scharning model and its generalisation with a kink are less pronounced.

Finally, it is informative to compare the failure time predictions obtained from the generalised model with no kink with predictions that have been made for this material using other modern extrapolation techniques recently published in the literature. In a recently published paper, Evans [17] applied the 4Θ projection technique and a Monkman–Grant representation of this technique to a data set on 1Cr–1Mo–0.25 V steel. In this representation, creep rates at low strains were used to predict minimum creep rates (a relation which is implied by the 4Θ methodology),

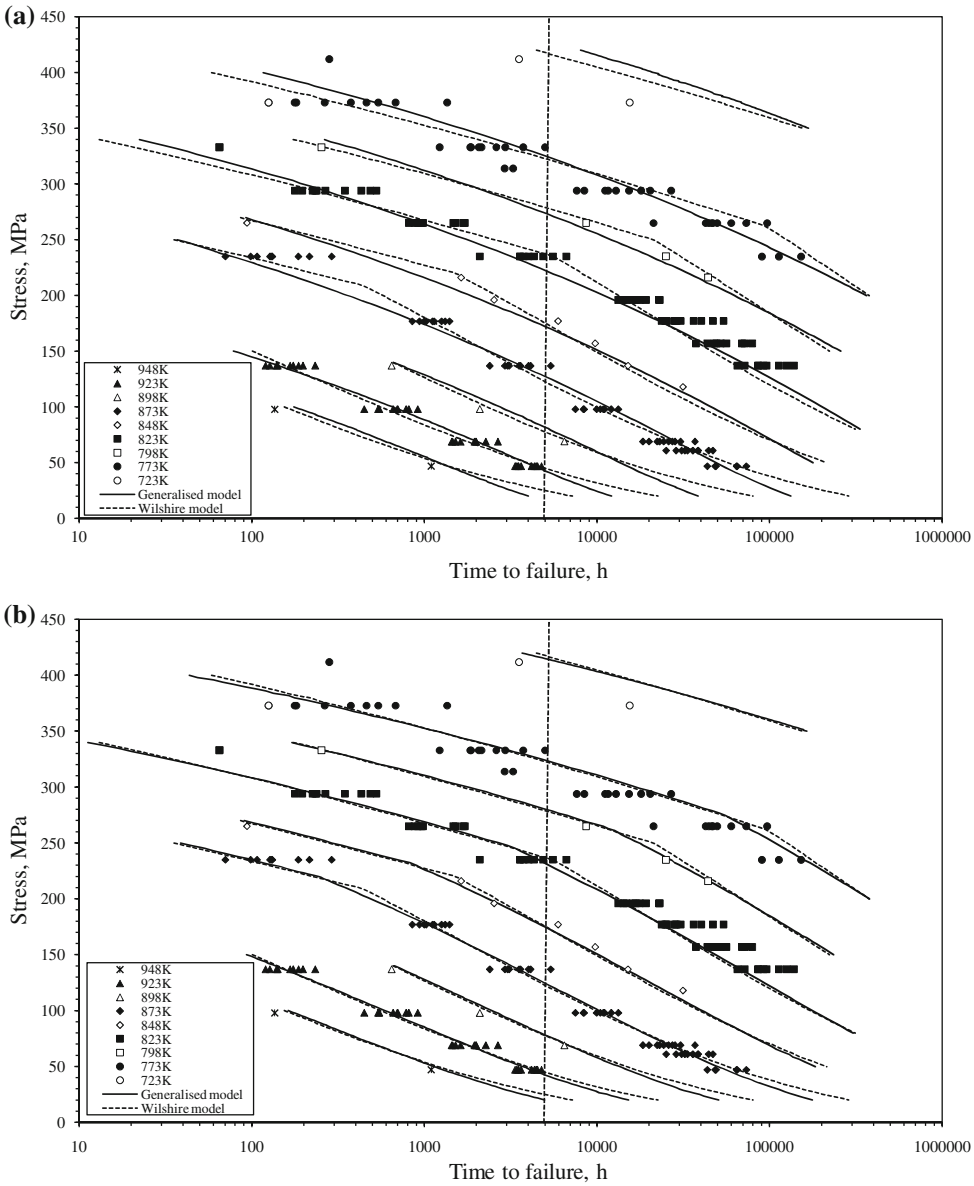

Fig. 6 Multi batch stress rupture data for 1Cr–1Mo–0.25 V steel at 723–948 K compared with predicted curves using the generalised model with (**a**) no kink of Eqs. 2a and 2b and the Wilshire–Scharning model of Eq. 4 and (**b**) a kink of Eqs. 2a and 6 and the Wilshire–Scharning model of Eq. 4

which in turn are used to predict failure times using the Monkman–Grant relation. These methods were applied to a much smaller data set than the NIMS data set used in this article, with models being estimated from test results varying between 14 and 4,500 h and extrapolations then being made out to 31,000 h.

Within this reduced timescale, the 4Θ projection technique produced a mean absolute percentage error (MAPE) in extrapolation of around 47%, with UM = 31%, UR = 62% and UD = 7%. Using strain rates and 0.5% strain to predict failure times, the MAPE = 26%, with UM = 1%, UR = 46% and UD = 53%. Bearing in mind that the above-generalised model with no kink was used to extrapolated out to over 100,000 h (not 31,000 h) this model had a MAPE = 28% with UM = 7%, UR = 1% and UD = 92%. Thus the generalised model with no kink produces a similar MAPE to the Monkman–Grant representation of the 4Θ technique—but over a much longer time sale—but this model has a much lower systematic component to these prediction errors.

Conclusions

A generalisation of the Wilshire–Scharning methodology has been put forward that has the potential to increase the predictive accuracy of the methodology—a property that will be so essential if it is to be adopted as a way of economising on the acquisition of long-term creep design data. A demonstration as to how this model can be estimated within Excel was also presented. When applied to 1Cr–1Mo–0.25 V steel it was found that the best

predictions of longer term times to failure were obtained using the generalised model with no kink. On average this model was in error by some 15,519 h or 1.8 years, but just as importantly nearly 92% of this error was random in nature. This generalisation was shown to give much more pessimistic lifetime predictions at lower stresses compared to the restriction implied by the Wilshire–Scharning model. Further, the generalised model with no kink produces a similar MAPE to the Monkman–Grant representation of the 4Θ techniques—but over a much longer time sale—but has a much smaller MAPE compared to the 4Θ technique. Just as important is the result that this model has a much lower systematic component to these prediction errors.

Areas for future work included comparing the Wilshire—Scharning methodology with the more traditional parametric models currently available within the literature using materials that will be required to raise efficiency and reduce fuel costs associated with future power generation (i.e. the austenitic steels such as stainless steel). The generalisation given above can also be further amended by allowing σ to vary with test conditions (i.e. essentially allowing creep variability to be a function of stress and temperature) and by allowing Q_c^* to be estimated from the data and modelled, perhaps, using a kinked function similar to one used for the stress relation.

References

1. Methods of extrapolation used in analysis of creep rupture data. ISO 6303, 1981
2. Yagi K (2005) In: Shibli IA et al (eds) Proceedings of the conference on creep and fracture in high temperature components-design and life assessment issues. DEStech Publ. Inc, London, p 31
3. Bendrick W, Gabrel J (2005) In: Shibli IA et al (eds) Proceedings of the conference on creep and fracture in high temperature components-design and life assessment issues. DEStech Publ. Inc., London, p 406
4. Kimura K (2005) In: Shibli IA et al (eds) Proceedings of the conference on creep and fracture in high temperature components-design and life assessment issues. DEStech Publ. Inc., London, p 1009
5. Cipolla L, Gabrel J (2005) In: Proceeding of the conference on super-high strength steels. Associazione Italia di Metallurgia, Rome, CD ROM
6. Wilshire B, Battenbough AJ (2007) Mater Sci Eng A A443:156. doi:10.1016/j.msea.2006.08.094
7. Wilshire B, Scharning PJ (2008) Mater Sci Technol 1:1. doi:10.1179/174328407X245779
8. Wilshire B, Scharning PJ (2008) Int Mater Rev 53(2):91. doi:10.1179/174328008X254349
9. Wilshire B, Scharning PJ (2008) J Mater Sci 43:3992. doi:10.1007/s10853-007-2433-9
10. Evans M (2008) Int Mater Rev (forthcoming)
11. NIMS Creep Data Sheet No. 9b, 1990
12. Stacy EW, Mihram GA (1965) Technometrics 7:349. doi:10.2307/1266594
13. Abramowitz M, Stegan IA (1965) Handbook of mathematical function. Dover, New York
14. Prentice RL (1965) Biometrika 62:607. doi:10.1093/biomet/62.3.607
15. Berndt B, Hall B, Hall R, Hausman J (1974) Ann Econ Soc Meas 3–4, 653
16. Theil H (1961) Economic forecasting and policy. North-Holland, Amsterdam
17. Evans M (2006) J Mater Sci 41:3907. doi:10.1007/s10853-005-5506-7